Nonisothermal Adsorption in Fixed Beds

OSCAR A. MEYER and THOMAS W. WEBER

State University of New York at Buffalo, Buffalo, New York

Removal of methane from a helium stream by adsorption on Columbia SXC activated carbon was studied experimentally and theoretically. A mathematical model for the process was developed and the governing differential equations were solved numerically. The model incorporates heat and mass transfer resistances within and around the adsorption particle. Wall effects and moderate heat loss to the surroundings are also included. The required heat and mass transfer correlations were obtained from the literature. Simple expressions were developed to determine the relative resistances for heat and mass transfer within and around the adsorption particles.

Fixed-bed adsorbers for gas separation present a frequent but difficult design problem for process engineers. These units are operated on a cycle of adsorption and regeneration steps, and estimation of the cycle time is the chief problem. The auxiliary operations such as bed switching, pressurization, depressurization, heating, and cooling, must be considered also, but these time requirements can be easily assessed.

The time of the adsorption step depends on the purity required for the effluent from the bed, the time of the regeneration will depend on how "clean" the bed should be before beginning the next adsorption step. Clearly, knowledge of the effluent concentration with respect to time is important.

The adsorptive capacity of a bed is the difference in loading between the end and the beginning of an adsorption step. In the most general case, the pounds of adsorbate per cubic foot of bed in these initial and final conditions will vary along the bed. And under dynamic conditions this loading will not be in equilibrium with the gas phase. With these stipulations an overall material balance of the adsorbate gives

$$G_F y_F t - \int_o^t G_E y_E dt = \int_o^{z_E} \rho_a (w' - w'_o)\, dz + (\alpha + \epsilon) \int_o^{z_E} (\rho y - \rho_o y_o)\, dz \quad (1)$$

The first term on the left is the total adsorbate fed to the bed and the second is the amount which has left the bed. On the right-hand side, the first term represents the amount of adsorbate adsorbed and the second is the adsorbate accumulated in the voids of the bed.

Equation (1) is not useful, since in a design problem, only the feed conditions are known. It could be used only if the effluent concentration history and the adsorbate distribution in the bed can be predicted. This has led to the development of mathematical models for describing the performance of a bed. The other approach toward solution of the problem has been through empirical correlations.

As an example of the empirical approach, Getty and Armstrong (5) studied air drying over activated alumina. To achieve a dew point of 0°F. for the effluent, the adsorption period was correlated with the contact time and feed conditions. The equations are easy to use, but the procedure has not been widely applied, because dynamic data for the specific system must be collected to develop the correlation.

MATHEMATICAL MODELS

The technique of mathematical modeling is merely the formulation of balances for conserved properties of the system: mass, energy, and momentum. These balances, in most problems, result in differential equations. If the model is correct the solution of these differential equations will describe the behavior of the system. In this paper the differential equations for heat and mass transfer are formulated and numerically solved. The data required for the model are the loading function, which is the equilibrium relationship between the gas and the solid, and the values of the rate coefficients for heat and mass transfer. While the loading function can be measured accurately enough, heat and mass transfer coefficients, especially in the porous solid, are difficult to measure and are not known accurately.

In an adsorption bed, containing a granular adsorbent, the processes occurring may be pictured as illustrated in Figure 1. The adsorbate is transferred from the bulk stream to the surface of the adsorbent and then by diffusion into the particle. During this diffusion the adsorbate equilibrates with the matter on the internal surface and heat is generated. This heat is removed from the particle into the gas stream from which it passes into the wall of the container and then into the surroundings. Due to the radial thermal gradient a radial concentration gradient also exists.

Two limiting cases are of particular interest: isothermal and adiabatic. If all heat transfer rates were infinite, then adsorption would be isothermal. In theory, this is not possible, but it is approached in a small-diameter, uninsulated bed where the thermal conductivity of the vessel wall is high and the residence time of the gas stream is large. A large residence time provides the time necessary for the removal of the heat of adsorption from the wall. If the heat transfer rate into the vessel wall is zero (step 8 in Figure 1), then the adsorption process is adiabatic. On the other hand, if the heat transfer rate in step 8 is finite, but the heat loss through the insulation is zero, then the process can be described as damped adiabatic,

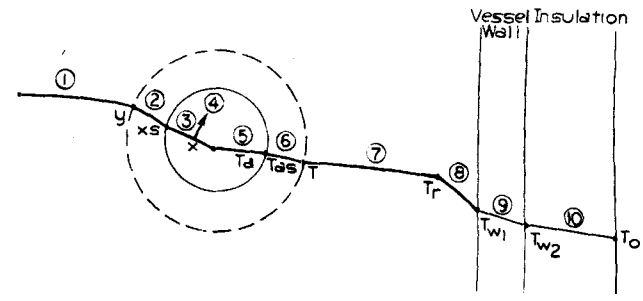

Fig. 1. Process steps in adsorption.

Oscar A. Meyer is at Monsanto Company, Sauget, Illinois.

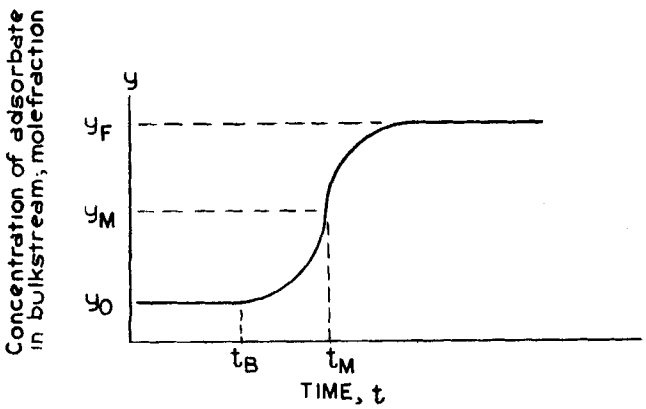

Fig. 2. Effluent concentration history curve.

which means that the amplitude of the temperature peaks is depressed by the regenerative heat capacity of the wall. Clearly, adiabatic operation is theoretically impossible.

The dynamic behavior of an adiabatic adsorption bed is frequently described by the movement and the shape of the temperature and concentration profiles as functions of time and position. Of course, one is strongly influenced by the other. If the bed operates nearly isothermally, only the concentration profile assumes importance. The effluent concentration history at the end of the bed, frequently termed the *breakthrough curve*, is usually of primary interest. It has three important properties: the breakthrough time, the lag time, and the sharpness.

The shape of a typical breakthrough curve is shown in Figure 2. As indicated, the breakthrough time t_B is that at which the effluent concentration just begins to increase from its initial value y_o. The initial value is of course dependent on the loading condition of the bed after regeneration. When the bed finally becomes completely saturated, the effluent concentration is that of the feed y_F. Arbitrarily, the lag time t_M is defined as the time required for the effluent concentration to reach the arithmetic average of the initial and final effluent concentrations. An index of the sharpness for the breakthrough curve is its slope at this average value of the concentration, that is, at the lag time.

The lag time is a measure of the holdup capacity of the bed. The sharpness of the breakthrough curve and the breakthrough time depend on the dynamics of the system. Resistance to mass transfer decreases the sharpness of the breakthrough curve as well as the breakthrough time. Similar effects are observed when the adsorption is not isothermal. Clearly, breakthrough curve with an infinite slope can never be achieved, it will always show some spread with respect to time.

THEORETICAL WORK ON THE ISOTHERMAL CASE

Most models for predicting the effluent concentration from an adsorption bed have been restricted to the isothermal case. Figure 1 shows that even for this case, there can be as many as three steps involved: steps 2, 3, and 4.

The differential equations describing the system have been handled analytically if the adsorption isotherm was linear and the variation of gas velocity along the bed could be neglected. These assumptions are valid only for dilute concentration of the adsorbate. The major differences between the various models proposed for the isothermal case lie in the resistance or combination of resistances to mass transfer.

The simplest model is that where there is no resistance to mass transfer. DeVault (*4*) and Glueckauf (*6*) developed this case for gas chromatography. This model has not been used as a design tool, but it has merit in the basic understanding that the breakthrough curve always has a leading and a trailing end. The breakthrough curve predicted by this model is described by an error function.

An increase in complexity occurs when one resistance to mass transfer is accounted for in the model. Hougen and Marshall (*7*) solved the case where the controlling resistance is external diffusion through the gas film surrounding the particles. The solution is in terms of Bessel functions. Rosen (*16*) and Thomas (*19*) solved the case where internal pore diffusion controls; Bohart (*3*) and Masamune and Smith (*12*) treated that case where the surface kinetics of adsorption controls.

The three possible two-resistance cases have also been solved by Masamune and Smith (*12*) and by Rosen (*16*). More recently, Masamune and Smith (*13*) have presented a solution to the three-resistance case as well.

The methods for solving the partial differential equations describing these several models have usually envolved multiple Laplace transformations. The resulting concentration profiles are expressed in terms of real improper integrals which are evaluated by numerical techniques.

Acrivos (*2*) pointed out that in the models the mass transfer resistance around and within the particles can be replaced by an axial diffusion term, because the existence of the mass transfer resistances will result in an axial dispersion. Unfortunately this procedure requires the use of a fictitious axial dispersion coefficient for which no correlations were proposed.

THEORETICAL WORK ON THE NONISOTHERMAL CASE

Only a few attempts are available in the literature for the nonisothermal case. Sanlaville (*17*) studied the heat and mass transfers for air drying over activated alumina and concluded that for short beds the process is controlled by the rate of heat transfer. Acrivos (*1*) outlined in a general manner the possibility of solution for adiabatic adsorption.

Leavitt (*9*) presented an analysis for cases where the mass transfer zone is stable; that is, the zone approaches a steady state length after an initial period of expansion. In addition to this important assumption, he also assumed that no heat is transferred through the bed wall. His treatment was broad enough to cover cases where there is a significant change in the superficial gas velocity as the adsorption proceeds in the transfer zone. The length of the mass transfer zone cannot be predicted by this method.

The most general treatment of the nonisothermal case to appear in the literature so far was a Ph.D. dissertation by Loechelt (*10*). Loechelt's model considered binary gas mixtures with no restriction on the concentrations of the adsorbable component. Overall heat and mass transfer coefficients between the gas and the pellets were employed. This amounts to assuming no radial temperature or composition gradients within a pellet. The theory was originally developed for an adiabatic system. For the adsorption column under test, heat losses were actually found to be significant and the model was revised. No special restrictions were placed on the form of the adsorption isotherm. The partial differential equations, four in number, were solved by numerical techniques on a digital computer. The model was tested with the use of a column, 2 in. in diameter and packed to a depth of 68 in. with activated carbon. An ethane–nitrogen mixture

was passed through the bed Considerable difficulties were encountered in matching the measured temperature and concentration profiles to those predicted by the model.

THE MODEL OF THIS RESEARCH

As an ultimate objective, it might be desirable to develop a model which incorporates all of the transfer mechanisms illustrated in Figure 1. Clearly, solution of such a case by analytical means would be impossible; solution by numerical means would be impractical. To make the model tractable, the following major assumptions were made:

1. The gaseous feed has only one adsorbable component.
2. Radial mixing is complete at a given cross section of the bed. Hence, there are no temperature or concentration gradients along the bed radius.
3. The kinetics of surface adsorption is fast and not controlling; this has been found to be true in most adsorption studies.
4. Axial conduction and diffusion are small compared to convective flow of heat and mass; therefore, they may be neglected.
5. Average transfer coefficients can be used throughout the course of the adsorption.
6. The pressure drop through the bed is negligible.

Mass and heat transfer resistances within and around the pellets are accounted for. The adsorption isotherms are not restricted to any special form. Heat transfer between the bed and the wall is included as well as heat losses from the wall to the surroundings.

There are six principal dependent variables. Four are functions only of time and axial position. These are: bulk velocity of the gas (v), bulk concentration of the gas (y), bulk temperature of the gas (T), and wall temperature (T_w). The other two variables are functions of time, axial position along the bed and radial position within a pellet. These are the adsorbent temperature (T_a) and the gas concentration in the pores (x). Secondary variables, which are functions of the principal variables, are the physical properties of the system.

It is convenient to divide the bed volume into three fractions. The bulk gas flows through the external void fraction (ϵ); the gas diffuses into the pores of the pellet in the intraparticle fraction (α). The actual solid portion comprises the remaining fraction (σ). It follows that

$$\alpha + \epsilon + \sigma = 1 \tag{2}$$

The partial differential equations for the model result from heat and mass balances taken around a differential length of the bed and the shell, with a differential width, of a single spherical particle. There are three mass balance and three heat balance equations. The complete derivations of the several equations are presented elsewhere (*14*); only the results are given here.

Within a particle, the concentration of adsorbate in the gas phase within a pore is described by

$$-\frac{1}{r^2}\frac{\partial}{\partial r}(r^2 N_1) = \frac{\partial(\rho_p x)}{\partial t} + \frac{\rho_a}{\alpha}\frac{\partial w}{\partial t} \tag{3}$$

The corresponding energy equation within the pellet is

$$\frac{(1-\epsilon)k}{\alpha r^2}\frac{\partial}{\partial r}\left(r^2\frac{\partial T_a}{\partial t}\right) - \frac{1}{r^2}\frac{\partial}{\partial r}\left[r^2\left(N_1\bar{H}_1 + N_2\bar{H}_2\right)\right] = \frac{\partial(\rho_p\bar{H})}{\partial t} + \frac{\rho_a C'_a}{\alpha}\frac{\partial T_a}{\partial t} + \frac{\rho_a}{\alpha}\frac{\partial(w\,u)}{\partial t} \tag{4}$$

In the bulk stream of gas within the bed, the material balance for the adsorbate is

$$-\frac{\partial(v\rho y)}{\partial z} - \frac{a\alpha}{\epsilon(1-\epsilon)}M_1 = \frac{\partial(\rho y)}{\partial t} \tag{5}$$

In Equation (5) the axial diffusion effects were neglected. An overall material balance takes on a similar form:

$$-\frac{\partial(v\rho)}{\partial z} - \frac{a\alpha}{\epsilon(1-\epsilon)}(M_1 + M_2) = \frac{\partial\rho}{\partial t} \tag{6}$$

Equation (6) describes the variation of gas velocity. The $\alpha/(1-\epsilon)$ factor prorates the mass flux for the exposed pore area of the adsorption particle. Due to reasons given later a slightly less rigorous expression is used in place of this equation to approximate the velocity variation. This relationship is obtained by assuming that the mass velocity of inert is constant; the resulting expression

$$v\rho\,(1-y) = \text{const} \tag{7}$$

Equation (7) incorporates velocity variation due to concentration and temperature changes. The energy balance in the bulk stream is

$$-\frac{\partial(v\rho H)}{\partial z} - \frac{a\alpha}{\epsilon(1-\epsilon)}[M_1H_1 + M_2H_2] - \frac{ah}{\epsilon}(T_{as} - T) - \frac{D_i\pi h_w}{\epsilon A}(T - T_w) = \frac{\partial(\rho H)}{\partial t} \tag{8}$$

The wall of the bed exchanges energy with the contents of the bed and with the surroundings through the insulation. The relatively small wall thickness of the bed allows the radial and axial heat conduction effects in the wall to be neglected. Thus, at any axial point the wall temperature is radially uniform and the axial heat conduction is negligible. The energy balance for the wall is

$$\frac{D_i\pi h_w}{m C_w}(T - T_w) - \frac{D_o\pi U}{m C_w}(T_w - T_o) = \frac{\partial T_w}{\partial t} \tag{9}$$

Before Equations (3) to (5) and (7) to (9) can be simultaneously solved, some of the terms must be defined. In Equations (3), (4), (5), and (8), the molar fluxes of the two components appear. Within the pores these may be related to the pore diffusivity (D) and the pore concentration (x) by

$$N_1 = -D\rho_p\frac{\partial x}{\partial r} + x(N_1 + N_2) \tag{10}$$

In a similar way, the molar fluxes from the bulk stream to the surface of the adsorbent are related to the mass transfer coefficient and the concentrations by

$$M_1 = k_f(y - x_s) + y(M_1 + M_2) \tag{11}$$

The mass fluxes of the inert component in these relationships are N_2 and M_2. Considering a single pellet, when it first comes into contact with gas containing adsorbate, we see that the flux of the adsorbate within a pore (N_1) is about equal but opposite in sign to the flux of the inert (N_2); similarly, the mass flux of the adsorbate from the bulk of the surrounding fluid (M_1) is about equal but opposite in sign to M_2. However, as the adsorption proceeds within the pellet, it is clear that N_2 and M_2 fall off in magnitude rapidly. Over a larger portion of the adsorption process for the pellet, N_2 is much smaller than N_1 and M_2 is much less than M_1. Hence, these fluxes of the inert component were neglected.

The enthalpies of the gas within the pores and in the bulk stream are related to compositions and temperatures by the equations:

$$\bar{H} = \bar{H}_1 x + \bar{H}_2 (1-x) \tag{12}$$

$$H = H_1 y + H_2 (1-y) \tag{13}$$

$$\bar{H}_i = C_{pi} (T_a - T_o) \; ; \qquad i = 1, 2 \tag{14}$$

$$H_i = C_{pi} (T - T_o) \; ; \qquad i = 1, 2 \tag{15}$$

The effective heat capacity of the adsorbent particles varies with the adsorbate loading w:

$$C_a = C'_a + w \frac{\partial u}{\partial T_a} \tag{16}$$

Since $(\partial u/\partial T_a)$ is the change in enthalpy of the adsorbed adsorbate with respect to temperature, it is a heat capacity (C_v). Then the total heat capacity of the bed is

$$C_a = C'_a + w C_v \tag{17}$$

The heat of adsorption is given by the isosteric heat of adsorption:

$$q = H_1 - u = -\frac{RT_a^2}{x} \left[\frac{\partial w/\partial T_a}{\partial w/\partial x} \right]_w \tag{18}$$

From the chain rule, if $w = w(T_a, x)$ we have

$$\frac{\partial w}{\partial t} = \frac{\partial w}{\partial T_a} \frac{\partial T_a}{\partial t} + \frac{\partial w}{\partial x} \frac{\partial x}{\partial t} \tag{19}$$

Upon substitution for the mass flux and accumulation of adsorbate in Equation (3), it becomes

$$\frac{1}{r^2} \frac{\partial}{\partial r} \left[r^2 \frac{\partial x}{\partial r} \right] = g_1 \frac{\partial x}{\partial t} + g_2 \frac{\partial T_a}{\partial t} \tag{20}$$

where

$$g_1 = \frac{1-x}{D \rho_p} \left[\rho_p + \frac{\rho_a}{\alpha} \frac{\partial w}{\partial x} \right]$$

$$g_2 = \frac{1-x}{D \rho_p} \left[\frac{\rho_a}{\alpha} \frac{\partial w}{\partial T_a} - x \frac{\rho_p}{T_a} \right]$$

Correspondingly, Equation (4) becomes

$$\frac{1}{r^2} \frac{\partial}{\partial r} \left[r^2 \frac{\partial T_a}{\partial r} \right] = g_3 \frac{\partial x}{\partial t} + g_4 \frac{\partial T_a}{\partial t} \tag{21}$$

where

$$g_3 = \frac{1}{(1-\epsilon)k} \left\{ \alpha \rho_p (C_{p1} - C_{p2}) (T_a - T_o) - \rho_a \frac{\partial w}{\partial x} \left[q - (1-x)(C_{p1} - C_{p2})(T_a - T_o) \right] \right\}$$

$$g_4 = \frac{1}{(1-\epsilon)k} \left\{ \alpha \rho_p C_p + \rho_a C_a - \rho_a \frac{\partial w}{\partial T_a} \left[q - (1-x)(C_{p1} - C_{p2})(T_a - T_o) \right] \right\}$$

During the development of Equations (20) and (21), products of derivatives appeared but they were found to be negligible in comparison with other terms in the equations; thus they were neglected. The details are reported elsewhere (*14*).

Equation (5) for the adsorbate concentration in the gas stream becomes

$$\frac{\partial y}{\partial t} + v \frac{\partial y}{\partial z} = -\frac{a \alpha k_f}{\epsilon (1-\epsilon) \rho} (y - x_s) \tag{22}$$

Finally, the energy equation for the bulk gas stream, Equation (8), takes the form

$$\frac{\partial T}{\partial t} + v \frac{\partial T}{\partial z} = \frac{1}{\rho C_p} \left\{ \frac{h a}{\epsilon} (T_{as} - T) - \frac{\pi D_i h_w}{\epsilon A} (T - T_w) - \frac{a \alpha k_f}{\epsilon (1-\epsilon)} (C_{p1} - C_{p2}) (T - T_o) (y - x_s) \right\} \tag{23}$$

The overall mass balance equation for the gas stream, Equation (7), and the energy equation for the wall, Equation (9), remain as were previously given. Hence, the system of six partial differential equations to be solved consists of Equations (20) to (23) and (7) and (9). The particle balances, Equations (20) and (21), are related to the macrobalances of the bed through the boundary conditions at the surface of the particle:

$$D \rho_p \left. \frac{\partial x}{\partial r} \right|_{r_s} = k_f (y - x_s) \Bigg\} \text{for all } z, t \tag{24}$$

$$-k \left. \frac{\partial T_a}{\partial r} \right|_{r_s} = h (T_{as} - T) \Bigg\} \tag{25}$$

Additional initial and boundary conditions imposed upon the solution are

$$\left.\begin{aligned} T(t, z) &= T(0, z) \\ T_w(t, z) &= T(0, z) \\ T_a(r, t, z) &= T(0, z) \\ x(r, t, z) &= y(0, z) \\ y(t, z) &= y(0, z) \end{aligned}\right\} \text{for } 0 \leq t \leq \int_0^z \frac{dz}{v} \tag{26-30}$$

$$\left.\begin{aligned} v(t, z) &= G_F/\epsilon \rho_F \\ T(t, z) &= T_F \\ y(t, z) &= y_F \end{aligned}\right\} \begin{aligned} &\text{at } z = 0 \\ &\text{for all } t \end{aligned} \tag{31-33}$$

$$\left.\begin{aligned} \frac{\partial x}{\partial r} &= 0 \\ \frac{\partial T_a}{\partial r} &= 0 \end{aligned}\right\} \text{for } r = 0 \tag{34-35}$$

SOLUTION OF THE EQUATIONS

Nonlinear partial differential equations have been solved sometimes by linearization followed by use of operational calculus. Certain special cases have been solved when small-order terms were neglected, yielding asymptotic solutions. In the present problem, these techniques could not be used, because a fairly general solution was desired. Therefore, the most general method, numerical solution, was employed.

Three of the partial differential equation, Equations (22), (23), and (9), can be reduced to ordinary differential equations along properly chosen characteristic lines. In Figure 3 a three-dimensional grid work is indicated and three natural characteristic paths of the system are defined.

Characteristic path	Definitive equation for characteristic path	Equation No. evaluated along characteristic path	Variable evaluated on characteristic path
I	$v = dz/dt$	(22), (23)	y, t
II	t = const.	(7)	v
III	z = const.	(9)	T_w

Additionally, at each axial position in the grid, there are two partial differential equations, Equations (20) and (21), of the parabolic form. These relate the temperature and composition within a spherical pellet to time and radial position. The whole computation scheme was built

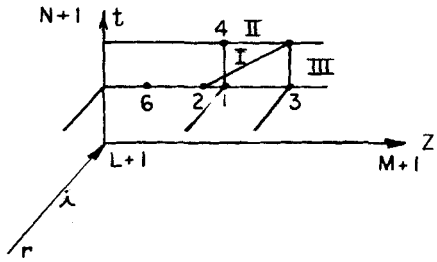

Fig. 3. Grid for numerical solution.

around these two equations. They were coupled to the bulk stream equations through the boundary conditions, Equations (24) and (25). Since the two pore equations are parabolic, the Crank-Nicholson technique was applied to each of them. Equations (9), (22), and (23) were all treated numerically by the implicit Euler formulation along their appropriate characteristics.

Referring to Figure 3, the three-space (r-t-z) was broken up into a three-dimensional grid consisting of L increments in the radial direction, M increments in the axial direction, and N increments on the time axis. As regards a typical point 5, the problem was to evaluate all six dependent variables at this point if conditions at points 1, 3, 4, and 6 were known. The conditions at point 2, needed in connection with characteristic I, could be approximated from those already known for points 1, 3, and 6.

At time zero, conditions were known all along the bed, that is, along the z axis. They were also known at all interior points of the pellets. Hence, conditions in the entire r-z plane were known. Also, the inlet conditions were known for all time, that is, along the t axis. The solution began at the entrance of the bed at the first time increment and proceeded in the z direction to the end of the bed. Thereafter, it jumped to the second time increment and moved axially again. This procedure continued until the end of the specified time period. The details are presented elsewhere (*14*).

Before the numerical computation can be started, the increments in the three-dimensional gridwork must be specified. One would use as large increments as the stability criteria of the system allow. Stability criteria for the time increments can be derived from the implicit Euler form of Equations (9), (22), or (23). The most rigid criterion is derived from Equation (23).

$$\frac{\Delta t}{2\,\epsilon\rho C_p A}\left[h\,a\,A + \pi\,D_i h_w\right] < 1 \qquad (36)$$

The axial increment size is specified from the inherent stability condition along characteristic path I.

$$\frac{\Delta z}{v\,\Delta t} \leq 1 \qquad (37)$$

There is no stability criterion for the radial increments because the Crank-Nicholson finite-difference forms of Equations (20) and (21) are unconditionally stable. If stability criteria of the system are satisfied, then convergence of the solution is also ensured. Of course, the unique convergence limit is not necessarily reached.

THE ADSORPTION EQUILIBRIUM

The system studied was a methane-helium gas mixture with Columbia SXC activated carbon as the adsorbent. This binary gas mixture was chosen because helium behaves as inert carrier only.

The adsorption isotherms were measured at four temperatures between 0° and 70°C. The results are shown graphically in Figure 4. It was necessary to correlate these data in an analytical expression suitable for machine computation. Redlich and Peterson (*15*) have suggested an expression for isotherms of the form:

$$w = \frac{p_1}{d + b p_1^{\,n}} \qquad (38)$$

where n is between 0 and 1. If n is 1, then this is the familiar Langmuir equation. The constants d and b are, of course, functions of temperature. The exponential term bp_1^n can be expanded into a polynomial, and if the higher than second-order terms are discarded, the result can be simplified to the form:

$$w = w_M \frac{\beta p_1}{1 + \beta p_1 (1 + \gamma p_1)} \qquad (39)$$

where

$$\begin{aligned} \beta &= \exp\,(a_1 + a_2/T_a) \\ w_M &= a_3 + T_a\,(a_4 + a_5 T_a) \\ \gamma &= a_6 + T_a\,(a_7 + a_8 T_a) \end{aligned}$$

The a_i's are constants. The data were fitted to this equation by nonlinear regression with the maximum neighborhood principle (*11*) incorporated. The values of a_i's are given in the Notation.

The loading function given by Equation (39) was used not only for calculation of the loading as function of temperature and pressure, but also for calculation of the isosteric heat of adsorption in accordance with Equation (18). The heat of adsorption was found to be about 7,500 B.t.u./lb.-mole and its variation with surface coverage was small.

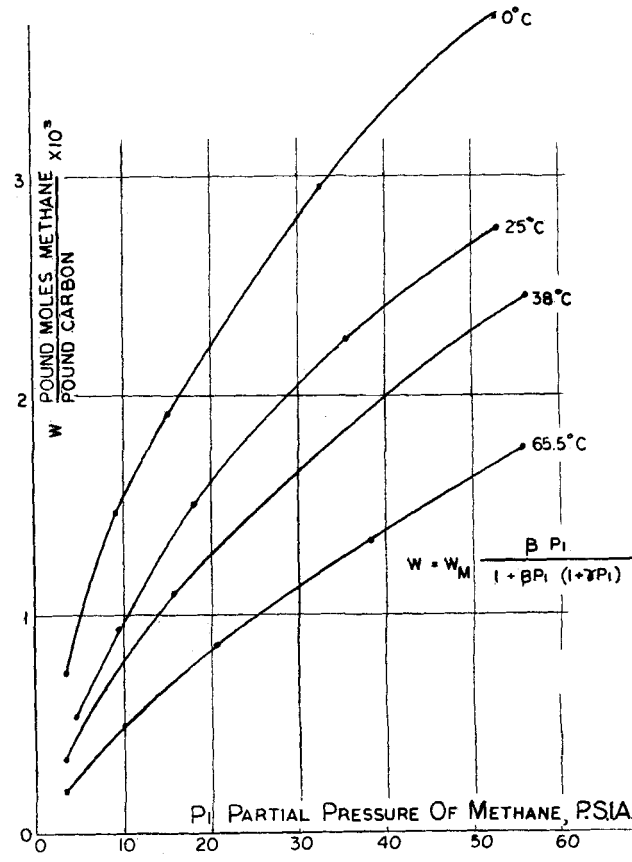

Fig. 4. Adsorption isotherms.

PROPERTIES OF THE ADSORBENT

The extruded activated carbon was manufactured by the National Carbon Company Fostoria, Ohio. The physical properties are:

Identification	SXC
Mesh size of particles	6/8
Average diameter, ft.	0.0104
Pellet density, g./cc.	0.716
Internal pore volume, cc./g.	0.934
Average pore diameter, Å.	14
Thermal conductivity, B.t.u./(hr.)(ft.)(°F.)	0.3
Specific heat, B.t.u./(lb.)(°F.)	0.2

The internal pore volume was measured by helium volume accommodation and the pellet density by volume replacement in mercury; these methods have been summarized by Smith and Howard (*18*). All other physical properties were supplied by the manufacturer.

TRANSFER RATE COEFFICIENTS

There are six transfer rate coefficients in this model. It was not the purpose of this study to measure these. Correlations are available for predicting most of them.

The coefficients of heat transfer (h) and mass transfer (k_f) between the gas and the surface of a pellet were evaluated from j factor correlations given in the charts of Hougen et al. (*8*). A correlation of Yagi and Wakao (*20*) was used to predict the coefficient of heat transfer (h_w) between the gas and the wall of the bed. The overall heat transfer coefficient (U) for the insulation was estimated from the thermal conductivity of the insulation and its thickness. The diffusivity in the pores was estimated by assuming that the mechanism was Knudsen diffusion. The last coefficient is the thermal conductivity of the adsorbent, which was supplied by the manufacturer.

Manipulation of the boundary conditions, at the surface of the pellets, indicated that for this system and operating conditions, nearly all of the resistance to mass transfer was inside the pellets, whereas the resistance to heat transfer was about equally divided between the inside and the outside of the pellets. The pertinent equations are

Fractional mass transfer resistance in the gas film:

$$\frac{1}{1+\dfrac{k_f r_s}{D\,\delta_p}} \tag{40}$$

Fractional heat transfer resistance in the gas film:

$$\frac{1}{1+\dfrac{h r_s}{k}} \tag{41}$$

EXPERIMENTAL EQUIPMENT

The apparatus used in these studies consisted of an adsorption bed with means for measuring the flow rates and compositions of the entering and leaving gas streams. Several temperatures were measured by thermocouples. A flow sheet of the equipment is shown in Figure 5.

The methane-helium feed passed through an orifice meter and through a flow controller. The orifice meter merely served as a check on the constancy of the gas flow rate. After passing through the bed, the flow was split. Most of the gas went directly to the gas meter; a small portion of the effluent passed through a Wilkens A-90-P2 gas chromatograph and then rejoined the main effluent stream before the gas meter. The vacuum pump was only used for regenerating the bed.

The Wilkens unit was operated without a separation column. The thermal conductivity cells in this model are of the diffusion type, with large ports so that the analysis was very

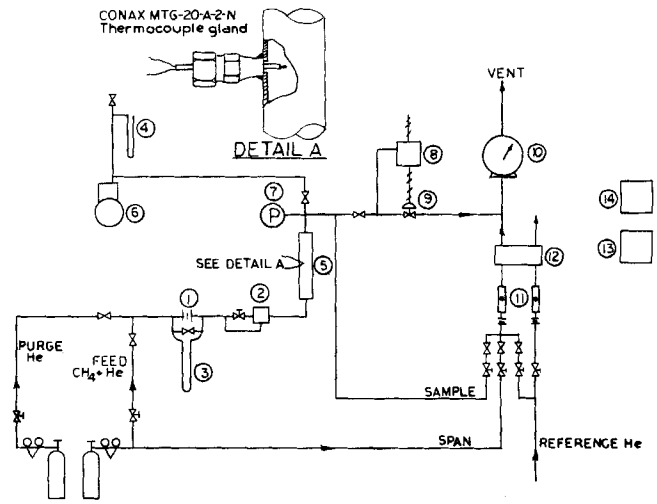

Fig. 5. Apparatus. *1*, orifice; *2*, flow controller; *3*, *4*, well type manometers; *5*, adsorption bed; *6*, vacuum pump; *7*, pressure gauge 400 lb./sq.in.; *8*, pressure controller; *9*, pressure control valve; *10*, gas meter; *11*, rotameter; *12*, gas analyzer; *13*, strip chart recorder; *14*, temperature recorder.

fast but flow sensitive. The analysis lag time, including the holdup of the lines, was estimated to be about 3 sec. The flow sensitivity of the cells was eliminated by inserting a 2-in. long capillary tube, 0.005 in. I.D., between the control valve and the flow indicating rotameter.

The first part of the experimental program concerned the measurement of the adsorption isotherms. In these runs, the bed consisted of a 10-ft. length of copper tubing, 0.5 in. O.D. and having a wall thickness of 0.035 in. Other properties of the bed (designated as bed No. 1) are presented in Table 1. The bed was wound into a coil about 16 in. in diameter and submerged in a constant-temperature bath. The temperature could be controlled to 0.1°C. Before entering the bed, the feed passed through a 7-ft. length of copper tubing which was also submerged in the bath. This served as a heat exchanger to bring the feed to the bed temperature before the gas came into contact with the adsorbent. Thermocouples at the inlet and outlet ends of the bed, as well as in the bath, indicated that isothermal conditions prevailed during all of these runs.

In the second part of the experimental work, runs were carried out to test the mathematical model. Bed No. 2, as described in Table 1, was used. Five thermocouples were placed inside the bed at points 2, 15, 30, 45, and 58 in. from the entrance of the bed. A sixth thermocouple measured the temperature of the surroundings. The bed was covered with a polyurethane foam insulation with a thickness of 0.8 in. and a thermal conductivity of 0.014 B.T.U./(hr.)(ft.)(°F.).

EXPERIMENTAL TEST OF MODEL

Five nonisothermal runs were made and the results were compared with those predicted by the model. As an illustration run 3 will be described, because the high methane con-

TABLE 1. CHARACTERISTIC DATA FOR THE ADSORPTION BEDS

Bed No.	1	2
Material of container wall	Copper	SS-304
Bed length, ft.	10.0	5.0
Bed O.D., in.	0.50	1.050
Wall thickness, in.	0.035	0.083
Weight of container wall, lb./ft.	0.198	0.857
Specific heat of wall, B.t.u./(lb.)(°K.)	0.182	0.195
Bulk density of adsorbent, lb./cu. ft.	26.3	28.1
Intraparticle void fraction	0.394	0.421
Interparticle void fraction	0.410	0.370
Specific surface area, sq. ft./cu. ft.	374.0	399.0

centration resulted in the largest temperature rise and the high flow rate provided highly dynamic conditions. Other experimental data are described elsewhere (*14*). Briefly, the operating conditions were

Total pressure, lb./sq.in.abs.	99.2
Feed rate F, lb.-moles/hr.	0.217
Mole fraction methane in feed y_F	0.143
Feed temperature T_F, °C.	27.2
Ambient temperature T, °C.	27.4
Inlet velocity v, ft./sec.	2.23

The lag time of the breakthrough curve, as previously defined, was observed after 0.024 hr. of the start of the experiment. The maximum temperature peak was observed at one-quarter of the bed and it was 9°C. These data are presented in Figures 6 and 7.

To test the model it should be shown that experimental observation and simulating calculations would result in an identical breakthrough curve and identical temperature peaks at given positions of the bed. To start the simulating calculations six transfer coefficients and the increments for the three-dimensional gridwork of the numerical solution had to be defined. The origin of the transfer coefficients was discussed before in this paper. The values of the coefficients are

Intraparticle diffusivity	$D = 0.058$ cu. ft./hr.
Thermal conductivity of adsorbent	$k = 0.54$ B.t.u./(hr.)(ft.)(°C.)
Mass transfer coefficient	$k_f = 9.0$ lb.-moles/(hr.)(sq. ft.)
Heat transfer coefficient in bulk stream	$h = 130$ B.t.u./(hr.)(sq. ft.)(°C.)
Heat transfer coefficient for the wall	$h_w = 50$ B.t.u./(hr.)(sq. ft.)(°C.)
Heat transfer coefficient for the surroundings	$U = 0.378$ B.t.u./(hr.)(sq. ft.)(°C.)

The number of radial increments was arbitrarily chosen as 8. The arbitrary selection of the radial increments was allowed, because the unconditionally stable Crank-Nicholson technique was applied for the solution in the radial space. The number of time increments were calculated as 15,000 from Equation (36) for an endurance of 0.03 hr. Equation (37) resulted in a requirements of 312 axial increments. This would have consumed a computer execution time of 40 hr. on an IBM 7044 machine. The machine cost allowed an execution time of 2 hr. only. Thus, the number of axial increments were reduced to 16. To eliminate stability problems during the numerical solution, the differential equation describing the bulk stream velocity, Equation (6), was replaced by an algebraic equation, Equation (7). This provided a stable and convergent, but not necessarily unique, solution.

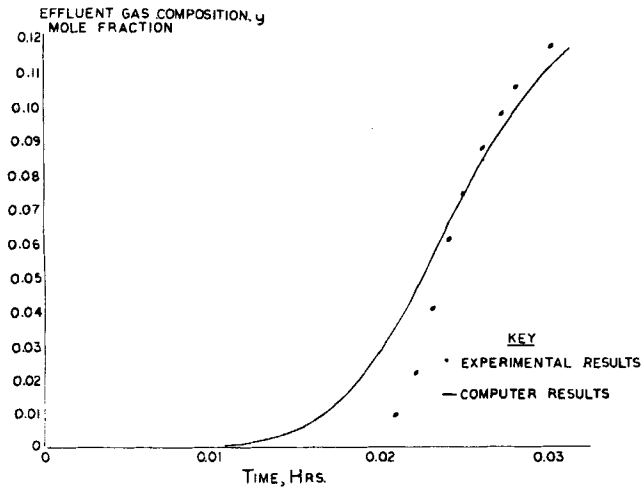

Fig. 6. Effluent concentration history.

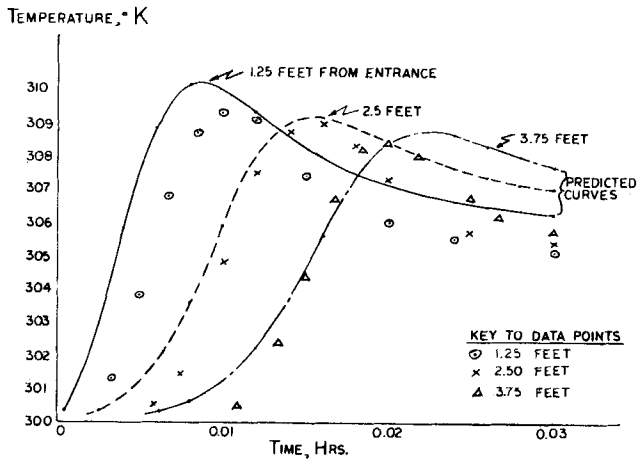

Fig. 7. Temperature profiles at three points.

The investigation of the transfer coefficients was beyond the scope of this research. Nevertheless, some remarks should be made on the validity of these coefficients. Quite extensive work has been done on the film transfer coefficients in packed beds and the used correlations (8) are recent summary of the art; therefore, the accuracy of the film transfer coefficients (h, k_f) is satisfactory. The thermal conductivity of the adsorbent was supplied by the manufacturer and therefore accepted. The heat transfer coefficient between the insulation and the surroundings (U) is not a significant parameter for well-insulated beds. Then the only disputable parameters are the pore diffusivity and the wall heat transfer coefficient.

In small simulated runs, the effects of the pore diffusivity and wall coefficients were studied. An increased value of the pore diffusivity resulted in a sharper breakthrough curve with increased lag time and also resulted in higher but sooner appearing temperature peaks.

The main effect of a larger value for the wall heat transfer coefficient was the suppression of the temperature peaks. During the computations it was noted that the results are sensitive to the variation of these parameters (D and h_w) and the value of h_w is correct within 30% and the pore diffusivity is within a factor of two. Better accuracy for these parameters cannot be claimed because the solution was a weak function of the size of the axial increments.

The results are shown in Figures 6 and 7. In Figure 6 the measured and predicted effluent concentration histories are compared. The dispersion of the predicted curve is significantly greater than that obtained experimentally. However, the lag times, as previously defined, are nearly the same. The greater dispersion of the predicted curve results to some extent from the rather large axial increments used. It should be noted, though, that the area to the left of the breakthrough curve represents the total dynamic loading of the bed at breakthrough. Clearly then, the predicted loading is about the same as experimentally observed.

In Figure 7, the measured and predicted temperatures are compared at several locations along the bed. The first curve, giving the temperature history at a point 1.25 ft. from the entrance, leads the measured values more than in the case for the other two locations, 2.5 and 3.75 ft. from the entrance. It should be pointed out, however, that even for the first curve, the discrepancy only amounts to around 5 sec. The predicted temperature rise exceeds the measured one at each location, but by one degree at most. The shapes of each predicted curve beyond its peak deviate rather significantly from the measured result. These discrepancies most likely result from the use of too large increments in the axial direction. This loss in accuracy had to be sacrificed for the twentyfold reduction in computer execution time.

Small simulated runs for the first quarter of the bed indicated that with smaller axial increments the predicted temperature profile approached the observed values. Since, the concentration profile was measured only after the full length of the bed, comparison for the concentration dispersion was not made.

SUMMARY

A mathematical model describing the dynamic behavior of a fixed-bed adsorber, operating at constant pressure, was developed. The model permits evaluation of bed performance even when the adsorption isotherms are not linear and the dynamics of the associated transfer processes cannot be neglected. A model of this complexity has never been solved yet.

The model is very general and not restricted by bed geometry, but its usefulness rests with the speed and cost of digital computers. This difficulty will be overcome with the introduction of the high precision hybrid computers. The salient points of this research are

1. With the time here for process simulation and mathematical modeling the state of art is still not capable of handling efficiently nonlinear systems.
2. Under highly dynamic conditions the heat and mass transfer zones are steadily expanding along the bed.
3. The use of the model is recommended for performance prediction in highly dynamic systems, where the residence time of the inert component is less than 1 sec. Systems with a long residence time can be predicted with one of the cited methods (*7, 9, 16*).
4. Considering the complexity of the adsorption system, especially the highly damped adiabatic nature (the mass of the vessel wall was fivefold greater than the mass of the packing), the authors feel that the agreement between experimental and model simulated runs is satisfactory.

FUTURE WORK

The computer program used to obtain the results presented here has already been changed in several ways to reduce the execution time. The final answer rests probably with the use of a hybrid computer. It is also planned to alter the model to handle the isothermal case.

The effective pore diffusivity is one of the most important parameters, yet its value is rather uncertain. Some studies on a differential bed could shed more light on this property and its dependence on temperature. If this technique should prove useful, it could be applied to other systems. The methane-helium mixture with activated carbon was not really a very severe test of the model. It would be interesting to apply the model to a system such as air drying by silica gel, where the heat effects are more pronounced. However, such a test would not be particularly worthwhile until better data are available on the effective pore diffusivity.

ACKNOWLEDGMENT

O. A. Meyer would like to thank the Allied Chemical Corporation and Linde Division of Union Carbide for financial support in the form of fellowships.

NOTATION

a = specific outside surface area of adsorbent, sq.ft./cu.ft. of bed
a_1 = $-0.989158\ 10^{1}$, dimensionless
a_2 = $0.192666\ 10^{4}$, °K.
a_3 = $-0.545930\ 10^{-3}$, lb.-mole/lb.
a_4 = $-0.726235\ 10^{-7}$, lb.-mole/(lb.)(°K.^{2})
a_5 = $0.371158\ 10^{-4}$, lb.-mole/(lb.)(°K.)
a_6 = $-0.541883\ 10^{-1}$, 1/lb./sq.in.abs.
a_7 = $0.305437\ 10^{-3}$, 1/(lb./sq.in.abs.)(°K.)
a_8 = $-0.444061\ 10^{-6}$, 1/(lb./sq.in.abs.)(°K.^{2})
A = empty cross-sectional area of bed, sq.ft.
C_a = heat capacity of the bed, defined by Equation (17), B.t.u./(lb.)(°K.)
C_a' = specific heat of adsorbent, B.t.u./(lb.)(°K.)
C_p = average specific heat of gas mixture, B.t.u./(lb.-mole)(°K.)
C_{p1} = specific heat of adsorbate, B.t.u./(lb.-mole)(°K.)
C_{p2} = specific heat of inert, B.t.u./(lb.-mole)(°K.)
C_v = specific heat of adsorbed adsorbate, B.t.u./(lb.-mole)(°K.)
C_w = specific heat of vessel wall, B.t.u./(lb.)(°K.)
D = intraparticle diffusivity, sq.ft./hr.
D_i = inside diameter of bed, ft.
D_o = effective outside diameter of bed for heat loss, ft.
G_E = mass velocity of bed effluent gas, lb.-mole/(hr.)(sq.ft.)
G_F = molar mass velocity of feed gas, lb.-mole/(hr.)(sq.ft.)
h = coefficient of heat transfer between particle and bulk stream, B.t.u./(hr.)(sq.ft.)(°K.)
h_w = coefficient of heat transfer between bulk stream and vessel wall, B.t.u./(hr.)(sq.ft.)(°K.)
H = enthalpy of bulk stream gas, B.t.u./lb.-mole
H_1 = enthalpy of adsorbate in the bulk stream, B.t.u./lb.-mole
H_2 = enthalpy of inert in the bulk stream, B.t.u./lb.-mole
$\overline{H}$ = enthalpy of gas in pores, B.t.u./lb.-mole
$\overline{H}_1$ = enthalpy of adsorbate in pores, B.t.u./lb.-mole
$\overline{H}_2$ = enthalpy of inert in pores, B.t.u./lb.-mole
k = effective thermal conductivity of adsorbent, B.t.u./(hr.)(ft.)(°K.)
k_f = mass transfer coefficient, lb.-mole/(hr.)(sq.ft.)
m = mass of vessel wall per unit length, lb./ft.
M_1, M_2 = molar flux of adsorbate and inert from bulk stream to outer surface of adsorbent, respectively, lb.-mole/(hr.)(sq.ft.)
N_1, N_2 = molar flux of adsorbate and inert in the pores of a particle, respectively, lb.-mole/(hr.)(sq.ft.)
p_1 = partial pressure of adsorbate, lb./sq.in.abs.
q = isosteric heat of adsorption, B.t.u./lb.-mole
r = radial position within a pellet, ft.
r_s = radius of spherical pellet, ft.
R = gas constant
t = elapsed time, hr.
t_B = breakthrough time, hr.
t_M = lag time, hr.
T = bulk stream temperature outside of film around particle, °K.
T_a = temperature of adsorbent, °K.
T_{as} = temperature of adsorbent at outer surface, °K.
T_F = bulk stream temperature at bed inlet, °K.
T_o = temperature of surroundings, °K.
T_r = bulk stream temperature, function of radial position in bed, °K.
T_w = temperature of vessel wall, °K.
u = enthalpy of adsorbate, B.t.u./lb.-mole
U = heat transfer coefficient between wall and surroundings, B.t.u./(hr.)(sq.ft.)(°K.)
v = interstitial velocity of the gas, ft./hr.
w = equilibrium adsorption loading, lb.-mole/lb. of adsorbent
w' = dynamic loading for bed, lb.-mole/lb. of adsorbent
w_o' = initial loading of bed, lb.-mole/lb. of adsorbent
w_M = constant in loading function, lb.-mole/lb. of adsorbent
x = mole fraction of adsorbate in pore of pellet
x_s = mole fraction of adsorbate at outer surface of particle
y = mole fraction of adsorbate in bulk stream
y_E = mole fraction of adsorbate in effluent gas
y_F = mole fraction of adsorbate in feed gas
y_o = mole fraction of adsorbate, at time zero, in bulk stream

y_r = mole fraction of adsorbate in bulk stream if radial gradient exists (See Figure 1)
z = axial position along bed, ft.
z_E = length of bed, ft.

Greek Letters

α = intraparticle void fraction, cu.ft./cu.ft. of bed
β = coefficient in loading function, 1/lb./sq.in.abs.
γ = coefficient in loading function, 1/(lb./sq.in.abs.)^2
ϵ = external void fraction, cu.ft./cu.ft. of bed
ρ_a = bulk density of adsorbent, lb./cu.ft. of bed
ρ_p = gas density in pores, lb.-mole/cu.ft.
ρ = gas density in bulk stream, lb.-mole/cu.ft.
ρ_F = density of feed gas, lb.-mole/cu.ft.
σ = solid fraction of bed, cu.ft./cu.ft. of bed

LITERATURE CITED

1. Acrivos, Andreas, *Ind. Eng. Chem.*, **48**, 703 (1956).
2. ———, *Chem. Eng. Sci.*, **13**, 1 (1960).
3. Bohart, G. S., and E. O. Adams, *J. Chem. Soc.*, **42**, 523 (1920).
4. DeVault, D., *J. Am. Chem. Soc.*, **65**, 532 (1943).
5. Getty, R. J., and W. P. Armstrong, *Ind. Eng. Chem. Proc. Design Develop.*, **3**, 60 (1964).
6. Glueckauf, E., *Trans. Faraday Soc.*, **51**, 34 (1955).
7. Hougen, O. A., and W. R. Marshall, *Chem. Eng. Progr.*, **43**, 197 (April, 1947).
8. Hougen, O. A., K. M. Watson, and R. A. Ragatz, "C.P.P. Charts," Wiley, New York (1960).
9. Leavitt, F. W., *Chem. Eng. Progr.*, **58**, 54 (Aug., 1962).
10. Loechelt, C. P., doctoral dissertation, Louisiana State Univ. (1964); Univ. Microfilm No. 65-3384, Ann Arbor, Mich.
11. Marquardt, D. W., *J. Soc. Ind. Appl. Math.*, **11**, 431 (1963).
12. Masamune, Shinobu, and J. M. Smith, *A.I.Ch.E. J.*, **11**, 34 (1965).
13. ———, *Ind. Eng. Chem. Fundamentals*, **3**, 179 (1964).
14. Meyer, O. A., doctoral dissertation, State Univ. New York, Buffalo (1966).
15. Redlich, O., and D. L. Peterson, *J. Phys. Chem.*, **63**, 1024 (1959).
16. Rosen, J. B., *Ind. Eng. Chem.*, **46**, 1590 (1954).
17. Sanlaville, J., *Gen. Chim.*, **78**, 102 (Oct., 1957).
18. Smith, R. C., Jr., and H. C. Howard, *Ind. Eng. Chem.*, **34**, 438 (1942).
19. Thomas, H. C., *J. Chem. Phys.*, **19**, 1213 (1951).
20. Yagi, Sakae, and Noriaki Wakao, *A.I.Ch.E. J.*, **5**, 79 (1959).

Manuscript received May 12, 1966; revision received September 22, 1966; paper accepted September 26, 1966.

Frequency Response of Gas Mixing in a Fluidized-Bed Reactor

LEONARD A. BARNSTONE and PETER HARRIOTT

Cornell University, Ithaca, New York

Frequency response methods were used to compare dynamic models for gas mixing and first-order reaction in a fluidized-bed reactor and for the experimental determination of interphase transfer characteristics. Theoretical predictions of frequency response characteristics were derived for two models based on the two-phase theory of fluidization. Experimental frequency response for a 1-ft. high bed were correlated better by a model based on perfect mixing in the dense phase than by a model based on plug flow in the dense phase. Excellent correlation was also obtained by a simple empirical model.

In recent years, there have been significant advances in understanding the nature of the fluidized state which have resulted in a plausible physical picture of fluidization embodied by the two-phase theory of fluidization. An excellent treatment of this theory and the experiments in support of it has been presented in a recent book by Davidson and Harrison (*2*). Several two-phase models have been presented in the literature to explain gas mixing and reaction kinetics in fluidized beds (*6* to *9*, *11*, *13*). In these models, mass transfer between the bubble and dense phases was accounted for in terms of an empirical interchange coefficient. The models differ mainly in the degree of mixing that is attributed to the dense phase; however, the two extremes of plug flow and complete mixing in the dense phase have not as yet been experimentally distinguishable.

It has not been possible to place great confidence on empirical correlations of interchange coefficients. Davidson and Harrison have developed a theory that can be used to predict interchange coefficients from bubble size, but this theory is presently of limited usefulness due to a lack of an empirical or theoretical method for predicting bubble size (*2*). Interchange coefficients have been determined experimentally from steady state measurements of a first-order reactions (*6* to *8*, *10* to *12*) and from step response mixing experiments with a tracer gas (*3*, *5*, *9*).

A more demanding test of the two-phase mixing models is to use them to predict the frequency response over a wide range of frequencies. The distinguishing features of such predictions can then be used for comparison of mod-

Leonard A. Barnstone is with Esso Research and Engineering Company, Florham Park, New Jersey.